Research article

Eutrophication decrease: Phosphate adsorption processes in presence of nitrates

Susana P. Boeykens [a, *], M. Natalia Piol [a, b], Lisa Samudio Legal [a], Andrea B. Saralegui [a], Cristina Vázquez [a, c]

[a] Universidad de Buenos Aires, Facultad de Ingeniería, Laboratorio de Química de Sistemas Heterogéneos (LaQuíSiHe), Buenos Aires, Argentina
[b] Universidad de Buenos Aires, CONICET, Argentina
[c] CNEA, Argentina

ARTICLE INFO

ABSTRACT

Eutrophication causes aquatic environment degradation as well as serious problems for different purposes of water uses. Phosphorus and nitrogen, mainly as phosphate and nitrate respectively, are considered responsible for eutrophication degradation.

The focus of this work was the study of adsorption processes for decreasing phosphate and nitrate concentrations in bi-component aqueous systems. Dolomite and hydroxyapatite were selected as low-cost adsorbents. Obtained results showed that both adsorbents have high capacity for phosphate adsorption which the presence of nitrate does not modify. Hydroxyapatite proved to be the most efficient adsorbent, however, it showed a low percentage of desorption and few possibilities of reuse. Dolomite, on the other hand, allows a desorption of the adsorbed material that favours its reuse.

© 2017 Elsevier Ltd. All rights reserved.

1. Introduction

Eutrophication of water bodies caused by the increased amount of nutrients has become a problem throughout the world (Manahan, 2001). This phenomenon produces aquatic environment degradation, either by changes in species composition, harmful algal blooms or bottom anoxia (Maier et al., 2009). It is a serious problem for different purposes of water uses (Anderson et al., 2002).

Nitrogen and phosphorus are two key elements responsible for the excessive increase of nutrients inducing aquatic plants growth. Although algae production is needed as a first link in the food chain of aquatic ecosystem, excessive growth under eutrophic conditions could eventually lead to a significant deterioration of the water body. Therefore, the first step for eutrophication acceleration is the entry of these nutrients in the aquatic system (Yang et al., 2008).

Phosphorus is an element that occurs naturally in water, however, certain human activities contribute significantly to its accumulation in water bodies. According to Von Sperling (2007), the natural origin of phosphorus compounds is due by the dissolution of soils compounds, the decomposition of organic matter and the cellular decomposition of microorganisms; its anthropogenic source is related to domestic and industrial wastes, detergents, animal excrement and fertilizers.

In the environment, the high concentration of nitrogen, as nitrates, not only favours the eutrophication of water bodies, but also produces very important implications for public health (Burkart and Stoner, 2002). The high nitrate concentration in drinking water is the main cause of methaemoglobinemia. Nitrates can be reduced to nitrites by intestinal bacteria and pass to the blood, producing the oxidation of Fe(II)-haemoglobin and making methaemoglobin unable to bind and carry oxygen to tissues (Eaton and Gilbert, 2008).

Adsorption processes have great potential as new technologies (Dabrowski, 2001). They are characterized by the use of cheap, non-toxic, biodegradable and reusable materials in some cases (Vanreppelen et al., 2013). Different combinations of contaminant/adsorbent under various experimental conditions have been studied (Fu and Wang, 2011). Both inorganic (Xu et al., 2008) and biomass materials (Miretzky et al., 2006) from different sources (Nhapi et al., 2011) have been used as natural adsorbents (Monoj

et al., 2015), especially modified (Cai et al., 2017) or synthesized (Huang et al., 2017). Some mineral materials were investigated for their capacities to adsorb phosphate (Johir et al., 2016; Coulibaly et al., 2016) and nitrate (Islam et al., 2010).

This study was focused on dolomite (sedimentary rock) and hydroxyapatite (bone meal) as adsorbents. Dolomite is a mineral that can be found in sedimentary layers several hundred feet thick, which is also found in metamorphic marbles, hydrothermal veins and replacement deposits. Hydroxyapatite is the major inorganic component of bone tissue of vertebrates (Anthony et al., 2011). The adsorbents selection was made taking into account their low costs and possibilities of reuse.

The search for selectivity in pollutant removal is the key to improving water treatment systems. The research with multi-component systems is an advance in the elucidation of the complexity of the problem which is not taken into account when working with simple systems. There are not many articles published on the investigation of competition between ions (Bia et al., 2012; Liu et al., 2013). The case of nitrate and phosphate is of great interest due to their concurrence in surface and underground waters (Chiban et al., 2012; Nodeh et al., 2017). For that reason, the focus of this work was the study of adsorption processes onto dolomite and hydroxyapatite, for decreasing phosphate and nitrate concentrations in bi-component aqueous systems.

Adsorption equilibrium and kinetics, structural and textural characterization of the adsorbents and desorption studies were performed to better understand these processes.

2. Materials and methods

The dolomite used as adsorbent in this research was obtained from quarry stone from Olavarría, Province of Buenos Aires, Argentine. The general formula is $AB(CO_3)_2$, where A can be calcium, barium or strontium, and B can be iron, magnesium, zinc or manganese. The hydroxyapatite ($Ca_5(PO_4)_3(OH)$) was obtained from bovine bones treated with dilute acid solutions and a subsequent pyrolyzing heat treatment, at 900 °C in oxydizing atmosphere for 2 h. Adsorbent samples were washed with distilled water, dried and sieved to a particle size between 53 and 74 μm.

Synthetic Phosphorous solution was prepared from a KH_2PO_4 (Mallinckrodt©) and the synthetic nitrate solution was prepared from KNO_3 (Mallinckrodt©), both salts were pre-dried at 105 °C for 1 h and dissolved with distilled water (APHA, 2012).

The pH of all the studied system was measured resulting, pH = 6.0 ± 0.5. Taking into account the speciation diagram of phosphoric acid, at the working pH, the main phosphate specie was di-acid phosphate (Liu et al., 2012).

The phosphorous concentration was determined according to the molybdovanadate method (APHA, 2012). Nitrate concentration was determined using a ion selective electrode (APHA, 2012).

2.1. Characterization of the adsorbents

The adsorbent textural properties were obtained from the determination of the nitrogen adsorption isotherms (at 77 K) employing the Brunauer-Emmett-Teller (BET) method (Gregg and Sing, 1982) with a Micromeritics, Gemini 2360 sortometer.

2.2. Dosage curves

Levels found in eutrophic lakes were taken into account to define the phosphate and nitrate concentrations of work. Considering that lakes can receive untreated wastewater or wastewater treated by conventional methods, they can contain up to 40 mg L^{-1} of nitrate and 30 mg L^{-1} of phosphate, according to Ansari and

Singh Gill (2014). It was decided to work with these maximum concentrations.

Dosage curves were performed in order to optimize the amount of adsorbent mass for removal phosphate and nitrate ions from a defined solution. For this purpose, different masses of the adsorbents were contacted in batch mode with 50 mL of the solution containing phosphate, nitrate or a mix of both, at pH = 6.0 ± 0.2. The systems were shaken at 200 rpm, for 24 h, at 25 ± 2 °C.

2.3. Adsorption isotherms

The experimental adsorption isotherms were performed measuring the residual phosphate concentration obtained from systems with different masses of adsorbents at constant phosphate concentration (30 mg L^{-1}) and phosphate in presence of nitrate (30 mg L^{-1} and 40 mg L^{-1}, respectively) with the same solution volume (50 mL) after 24 h of contact.

The total adsorption capacity (mg phosphate/g adsorbent) was calculated by equation (1):

$$q_a = \frac{C_a V}{m} \tag{1}$$

where, q_a (mg g^{-1}) is the adsorption capacity, C_a (mg L^{-1}) is the phosphate adsorbed concentration, m (g) is the adsorbent mass, and V (L) is the volume of adsorption solution.

2.4. Kinetics

The adsorption kinetic curves were performed in batch experiments for the different systems: 3.000 ± 0.002 g of dolomite or 0.6000 ± 0.002 g of hydroxyapatite with 50 mL of phosphate solution (30 mg L^{-1}) or phosphate and nitrate solution (30 mg L^{-1} and 40 mg L^{-1}, respectively). The residual phosphate and nitrate concentrations were measured at different times. The equilibrium times were defined when residual concentrations remain constant.

2.5. Equilibrium and kinetic models

In order to investigate the mechanism of adsorption processes, experimental data were fitted according to both, Langmuir and Freundlich models.

The proposed equation by Langmuir (1918) applies physical and chemical adsorption, and can be used to describe the equilibrium conditions for different adsorbate/adsorbent systems. The Langmuir equation is given by equation (2):

$$q_e = \frac{q_m b C_e}{1 + q_m C_e} \tag{2}$$

where, q_e (mg g^{-1}) is the amount of adsorbed species per unit mass of adsorbent at the equilibrium state, C_e (mgL^{-1}) is the concentration of the solution at the equilibrium state, q_m (mg g^{-1}) and b (L mg^{-1}) are Langmuir constants related to the maximum capacity and energy of adsorption, respectively.

The Freundlich model (1906) (equation (3)) assumes that the adsorption should be purely a physical process without change in the configuration of molecules.

$$q_e = K_f C_e^n \tag{3}$$

where, K_f and n are parameters related to the adsorption capacity and intensity, respectively.

For fitting experimental data obtained in the kinetic assays, pseudo-first order and pseudo-second order models were

employed.

The mathematical expression for the kinetics of pseudo-first order (Lagergren, 1898) is widely used for adsorption studies of liquids. The linear form is equation (4):

$$\ln(q_e - q_t) = ln q_e - k\, t \tag{4}$$

where q_t (mg g^{-1}) is the amount of adsorbed solute at time t, and k (min^{-1}) is the constant velocity.

The pseudo-second order model was developed by Ho and McKay (1999). It is assumed that sorbate is adsorbed on two active sites on the sorbent. The process can be expressed in a linear form by equation (5):

$$\frac{t}{q_t} = \frac{1}{k_s q_e^2} + \frac{1}{q_e} t \tag{5}$$

where, k_s (mg g^{-1} min^{-1}) is the velocity constant of pseudo-second order. The term ($k_s q_e^2$) represents the initial adsorption rate.

For obtaining the fitting parameters, OriginPro 8.5.1® software package was used.

2.6. Desorption studies

In this case, desorption experiments are performed in order to establish the possibilities of the adsorbent reuse, and how many useful cycles it can operate.

Analogously to the recovery of an ion-exchange resin, for recovering the exhausted adsorbent, desorption should be carried out with a saturated solution of a salt, or a strong base or acid which is more efficient for the displacement of the adsorbed ion.

Desorption efficiencies of the following solutions were evaluated: NaOH 0.1 M (pH = 12), NaCl 0.1 M (pH = 5), HCl 0.1 M (pH = 2) and distilled water (pH = 6.5).

For the experiments, a measured mass of five samples of each adsorbent loaded with phosphate were stirred with 50 mL of desorbent solution for 24 h.

Desorption percentage was calculated by equation (6):

$$Desorption(\%) = 100\left(\frac{C_d V_d}{q_a m}\right) \tag{6}$$

where C_d (mg L^{-1}) is the ion concentration in the desorbed solution, V_d (L) is the volume of the desorption solution, q_a (mg g^{-1}) is the adsorption capacity, and m (g) is the adsorbent mass. In all cases the initial solution of phosphate was 30 mg L^{-1}.

The desorption capacity, q_d (mg phosphate/g adsorbent), was calculated by equation (7):

$$q_d = \frac{C_d V}{m} \tag{7}$$

where, q_d is the desorption capacity (mg g^{-1}), C_d is the phosphate desorbed concentration (mg L^{-1}), m is the adsorbent mass (g) and V is the volume of desorption solution (L).

2.7. Fourier transform - infrared spectrometry studies

In order to investigate structural modifications in chemical functional groups due to the adsorption process, both adsorbents were analyzed before and after the experiments using a Fourier Transform Infrared Spectrometer (FT-IR Nicolet 8700). The characteristic absorption bands of the different functional groups were adjudicated by studying the spectrum obtained and comparing them with those described in the bibliography (Silverstein et al., 2005).

Table 1
Textural parameters for the dolomite and hydroxyapatite (S_{BET} is the BET superficial specific area and V_T is the total pore volume).

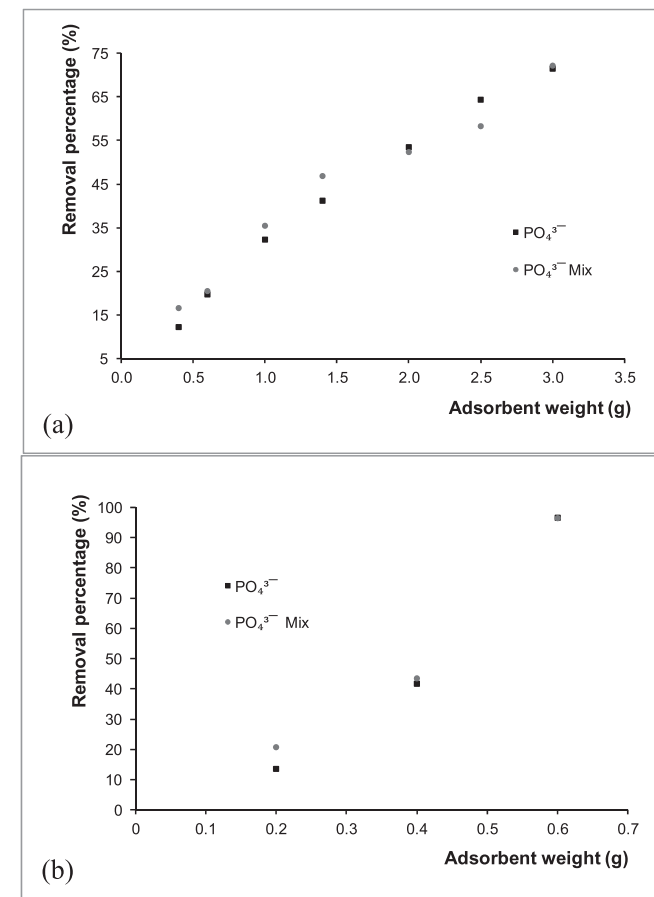| Adsorbent	S_{BET} (m^{2}g^{-1})	V_T (cm^{3}g^{-1})
Dolomite	1.83	0.0030
Hydroxyapatite	1.5	0.0044

Fig. 2. Dosage curves for phosphate (◆) and for phosphate + nitrate (●) (30 mg L^{-1} and 40 mg L^{-1}, respectively) onto: (a) dolomite, and (b) hydroxyapatite.
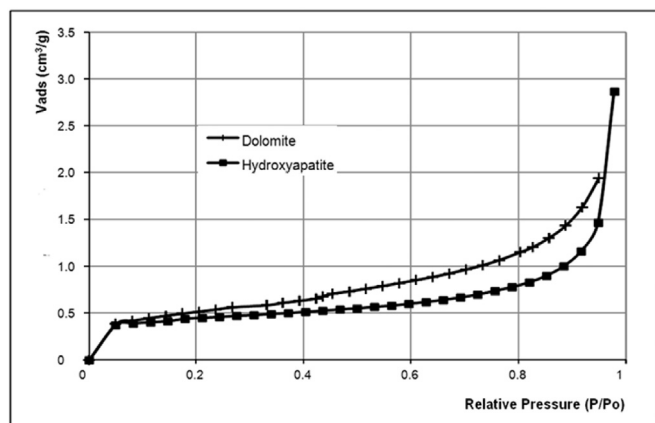

Fig. 1. Nitrogen adsorption isotherms of dolomite and hydroxyapatite powders (V$_{ads}$ is the adsorbed volume of nitrogen per unit mass of adsorbent).

3. Results and discussion

3.1. Characterization of the adsorbents

Fig. 1 shows the experimental nitrogen (77 K) adsorption isotherms obtained. Table 1 shows the textural parameters calculated from the adsorption isotherms for the two studied adsorbents employing the Brunauer-Emmett-Teller (BET) method.

The low value of the BET specific surface area and the total volume of pores suggest that these materials have not developed porosity accessible to nitrogen, therefore, it could be inferred that it is a non-macroporous sample. The value of the dolomite surface area found in this study is higher than that found by Mangwandi et al. (2014) and Karaca et al. (2006), which was 0.14 m^2/g. Comparatively, the specific surface of the dolomite is larger than that of the hydroxyapatite, however, the total pore volume is smaller. This may be due to the fact that the dolomite pores are smaller and can also be seen as a more homogeneous surface.

3.2. Dosage curves

In Fig. 2, the dosage curves for phosphate and for phosphate in presence of nitrate onto dolomite and hydroxyapatite are presented. The plot points are the average of at least three experiments.

For both adsorbents, the amount of adsorbed phosphate increased with the adsorbent mass. However, nitrate adsorption was not observed. It must be noted that the presence of nitrate does not modify the amount of adsorbed phosphate neither onto dolomite nor hydroxyapatite. The higher removal percentage for phosphate was obtained using hydroxyapatite systems. Dolomite and hydroxyapatite showed high adsorption capacity for phosphate even in the presence of nitrate.

Taking into account the range of phosphate and nitrate concentrations already defined, these results defined the appropriate adsorbent dose: 3 g for dolomite and 0.6 g for hydroxyapatite.

3.3. Adsorption isotherms

Isothermal studies were performed for systems with phosphate, and phosphate in presence of nitrate onto dolomite and hydroxyapatite. Fig. 3 shows the experimental adsorption isotherms (removed adsorbate concentration per gram of adsorbent at equilibrium (q_e) vs the remaining adsorbate concentration in the aqueous solution (C_e)). The plot points are the average of at least

Table 2
Isotherm parameters for phosphate adsorption onto dolomite and hydroxyapatite.

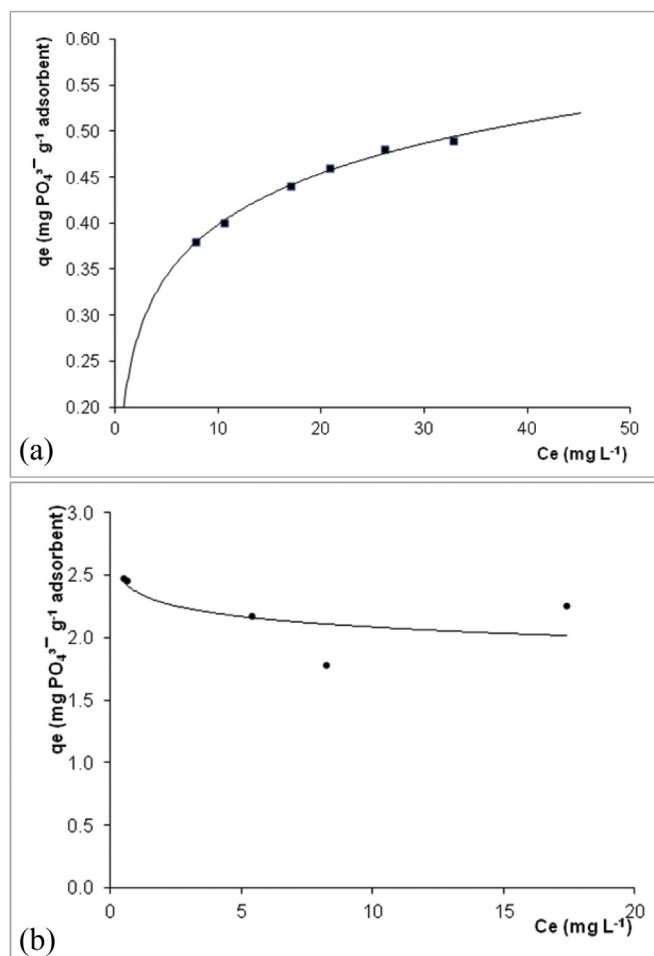| Adsorbent	Langmuir			Freundlich		
	q_m (mg/g)	b	R^2	n	K_f	R^2
Dolomite	0.30	0.30	0.9923	3.21	0.10	0.9175
Hydroxyapatite	1.10	3.53	0.9828	17.7	1.17	0.4327

Fig. 3. Experimental adsorption isotherms for phosphate onto: a) dolomite and b) hydroxiapatite.
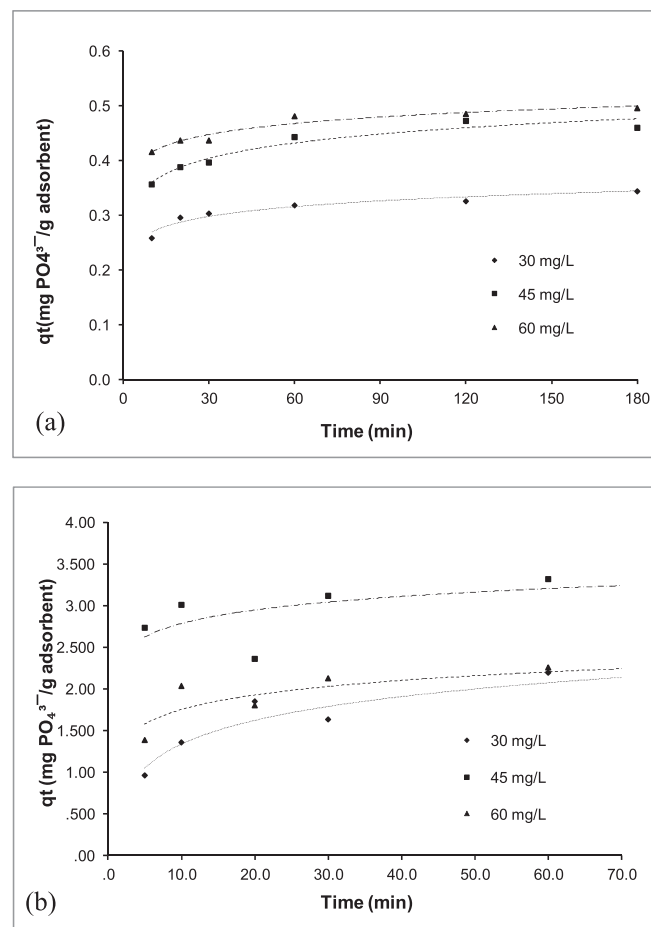

Fig. 4. Experimental kinetics curves for phosphate adsorption onto: (a) dolomite and (b) hydroxyapatite.

Table 3
Kinetics parameters for phosphate adsorption onto dolomite.

Initial phosphate concentration	$q_{e(exp.)}$ (mg/g)	Pseudo-first order model			Pseudo-second order model		
		q_e (mg/g)	k (min^{-1})	R^2	q_e (mg/g)	k_s	R^2
30	0.17	0.034	0.0122	0.834	0.167	0.0021	1
45	0.24	0.077	0.0270	0.985	0.246	0.0007	0.9991
60	0.25	0.043	0.0193	0.863	0.248	0.0015	0.9996

Table 4
Kinetics parameters for phosphate adsorption onto hydroxyapatite.

Initial phosphate concentration	$q_{e(exp.)}$ (mg/g)	Pseudo-first order model			Pseudo-second order model		
		q_e (mg/g)	k (min^{-1})	R^2	q_e (mg/g)	k_s	R^2
30	1.13	0.807	0.0496	0.9096	1.212	0.0959	0.9949
45	1.73	0.465	0.0287	0.6694	1.782	0.1283	0.9947
60	1.14	0.446	0.0562	0.8758	1.175	0.2468	0.9988

three experiments. It is important to note that the equilibrium results do not present significant differences between working with mono- or bi-component systems.

According to Sepúlveda et al. (2008), the shape of the adsorption isotherms, being convex or concave, could allow classify them as unfavorable or favorable, respectively. This is a general classification based on pure visual observation of experimental data (shape and curvature) for the adsorption isotherm (Hinz, 2001). In Fig. 3, onto dolomite, the adsorption process appear to be favorable, and for the hydroxyapatite, unfavorable.

Fitting parameters from Langmuir and Freundlich models obtained from experimental data are shown in Table 2.

The Langmuir model fits satisfactorily the experimental data from phosphate adsorption onto both tested adsorbents. Similar results were obtained for phosphate adsorption onto Mg-Al and Zn-Al in layered doubled hydroxide (Yang et al., 2014), onto nanocrystalline akaganéite and hybrid surfactant-akaganéite (Deliyanni et al., 2007), onto alkaline fly ash (Cheung and Venkitachalam, 2000), and onto mesoporous ZrO_2 (Liu et al., 2008). Another report shows a higher adsorption capacity of phosphate onto dolomite but at pH = 2 (Mangwandi et al., 2014).

The q_m parameter (adsorption capacity) obtained from fitting Langmuir model for dolomite is lower than that for hydroxyapatite, both results are similar to the experimental obtained values. This is consistent with the results of dosage; hydroxyapatite has the highest capacity of phosphate adsorption. The b parameter related to the binding energy between the phosphate and the adsorbent describes the same situation: it is more than ten times higher for hydroxyapatite-phosphate than for dolomite-phosphate.

The Freundlich model fits satisfactorily the experimental data only from phosphate adsorption onto dolomite. This is due to the unfavorable form of the isotherm for hydroxyapatite, Freundlich's model is unable to recognize such behavior.

3.4. Adsorption kinetics

The kinetics of the phosphate adsorption process was studied using the pseudo-first and second order models. Graphics are shown in Fig. 4 and the obtained parameters are listed in Tables 3 and 4. Satisfactory correlation coefficients were obtained for second-order model. This suggests the rate-limiting step could be a chemical sorption process.

The experimental adsorption capacities (q_{max}) for phosphate were 0.25 mg g^{-1} onto dolomite and 1.2 mg g^{-1} onto hydroxiapatite. For both adsorbents, phosphate adsorption was quite rapid; the equilibrium time was achieved after 60 min.

The high values obtained for R^2 ($R^2 > 0.99$) evidence the ability of the pseudo second-order model to represent the experimental results with a higher degree of accuracy in both systems. Besides,
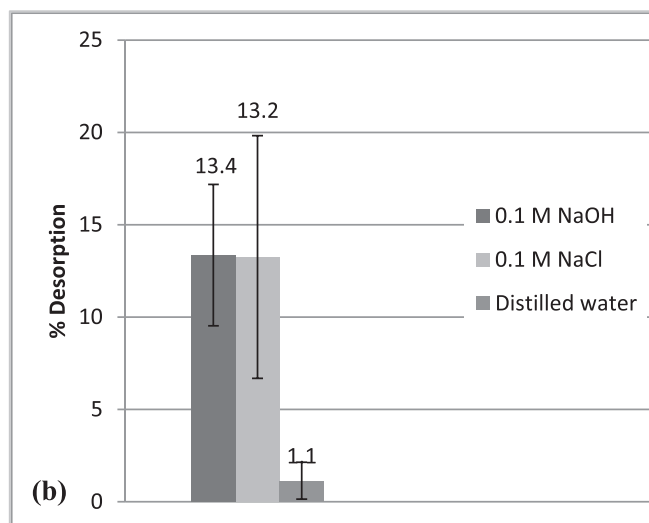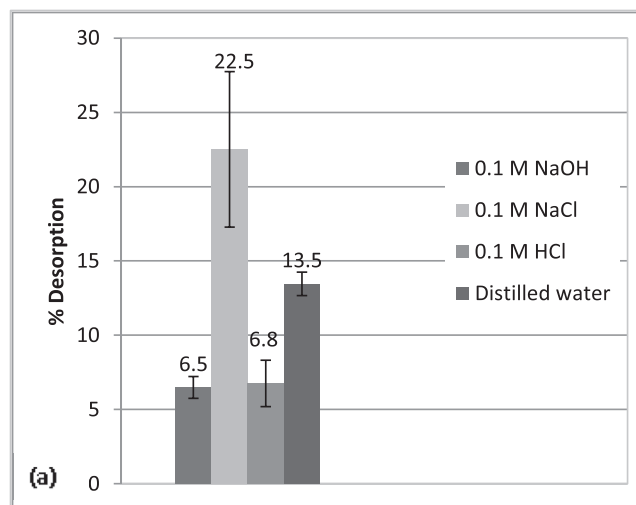

Fig. 5. Desorption efficiencies of various reagents for removing phosphate from: a) dolomite and b) hydroxyapatite.
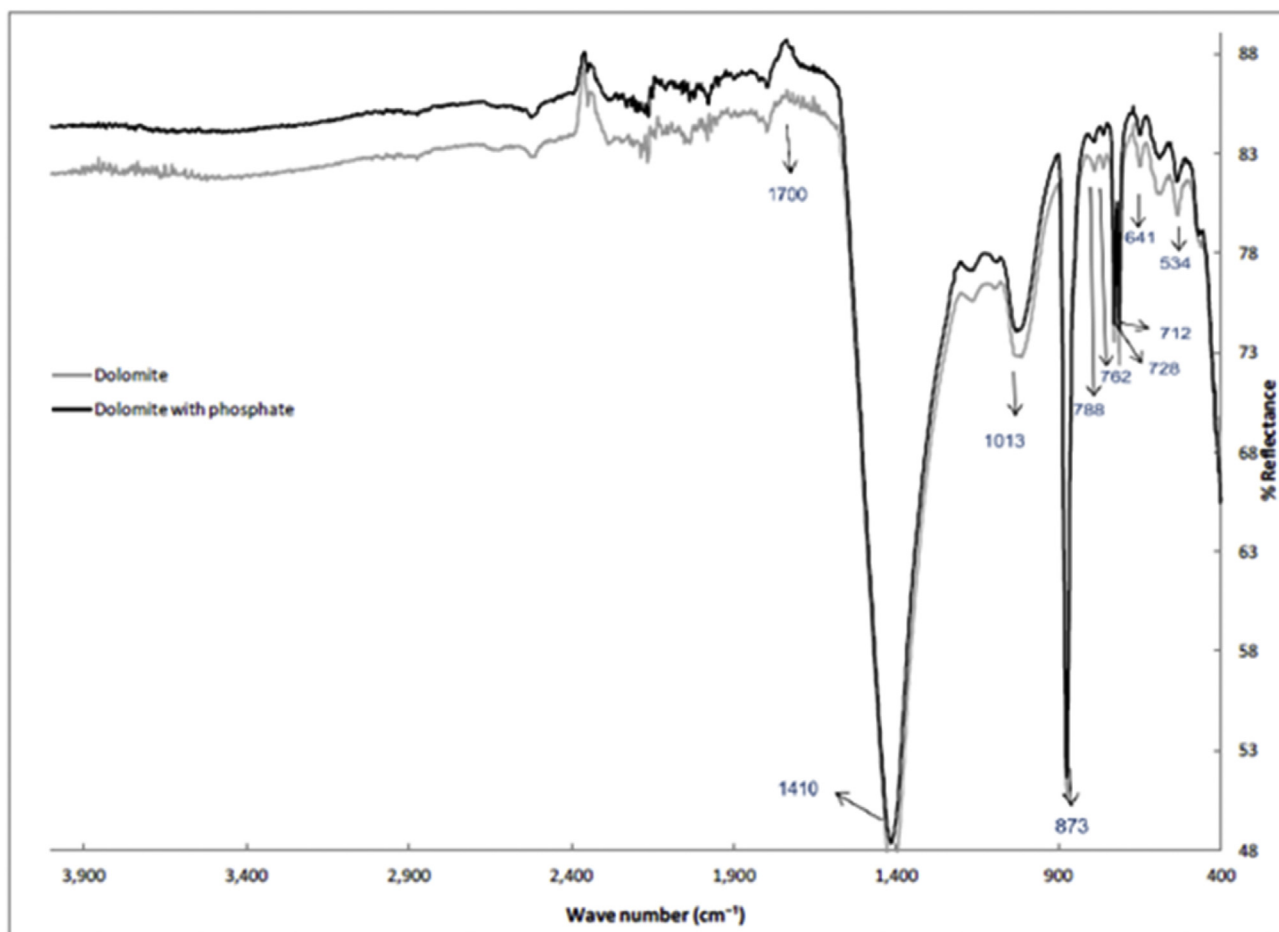
Fig. 6. FT-IR spectra obtained for dolomite with and without phosphate adsorption.

the q_e values calculated from the pseudo second-order model were close to the experimental values. It was found that the initial adsorption rate ($k_s q_e^2$) increases with the initial concentration. The non-linear relation between the rate constants and the initial concentrations indicates that mechanisms such as ion exchange and physical adsorption are involved in the process (Kumar et al., 2010).

3.5. Desorption studies

A summary of the desorption experiments results are presented in Fig. 5.

Dolomite desorption efficiency (%) of different desorbent solutions resulted in the following order: 0.1 M NaCl > distilled water > 0.1 M HCl > 0.1 M NaOH.

In the case of hydroxiapatite, the desorption percentages obtained by NaOH and NaCl are quite similar: 13.4 and 13.3%, respectively. It is further noted that the use of HCl caused the partial solubilization of the adsorbent, so it is discarded as desorbent. This reaction is due to the fact that the hydroxyapatite is formed mainly by calcium phosphate, which dissolves in acid. The acid exerted an aggressive effect on the structure of the hydroxyapatite, resulting in a gradual destruction (solubilization) of its components. This also explains the result obtained with Dolomite (mainly calcium carbonate) that the concentration of phosphate in solution is greater than the amount of phosphate adsorbed in the original sample.

Due to the desorption efficiency obtained, the NaCl solution was

selected for subsequent reuse cycles, for both adsorbents.

Desorption capacity of NaCl resulted in 0.035 mg of phosphate per gram of dolomite and 0.10 mg of phosphate per gram of hydroxyapatite. With other desorbents tested, desorption from both adsorbents resulted lower than 0.020 mg g^{-1}.

3.6. FTIR spectra

To better understand the adsorption process FTIR spectra were obtained from both adsorbents before and after this process.

In Fig. 6 the FT-IR spectra obtained from dolomite with and without phosphate are shown. After adsorption of phosphate, it was observed a slight decrease in the intensity of the bands at 1410 cm^{-1} (CO_3^{2-}). The tendency of these changes indicates interaction between surface groups present on the dolomite with phosphate. The intensity reduction of CO_3^{2-} bands could indicate the substitution of some carbonate groups in the dolomite by phosphates as was indicated previously by other authors (Albadarin et al., 2012; Kumar et al., 2010). There was an increase in the intensity of O-H group around 1700 cm^{-1} band, which can be attributed to the attraction between the O-H groups and phosphate ions, ie, electrostatic attraction. Calcium phosphate precipitate could be formed and phosphate could be also fixed with magnesium ion, in an amorphous form as it was suggested by Mangwandi et al. (2014).

Fig. 7 shows the IR spectra obtained from hydroxiapatite with and without phosphate adsorption. In the hydroxyapatite spectra,
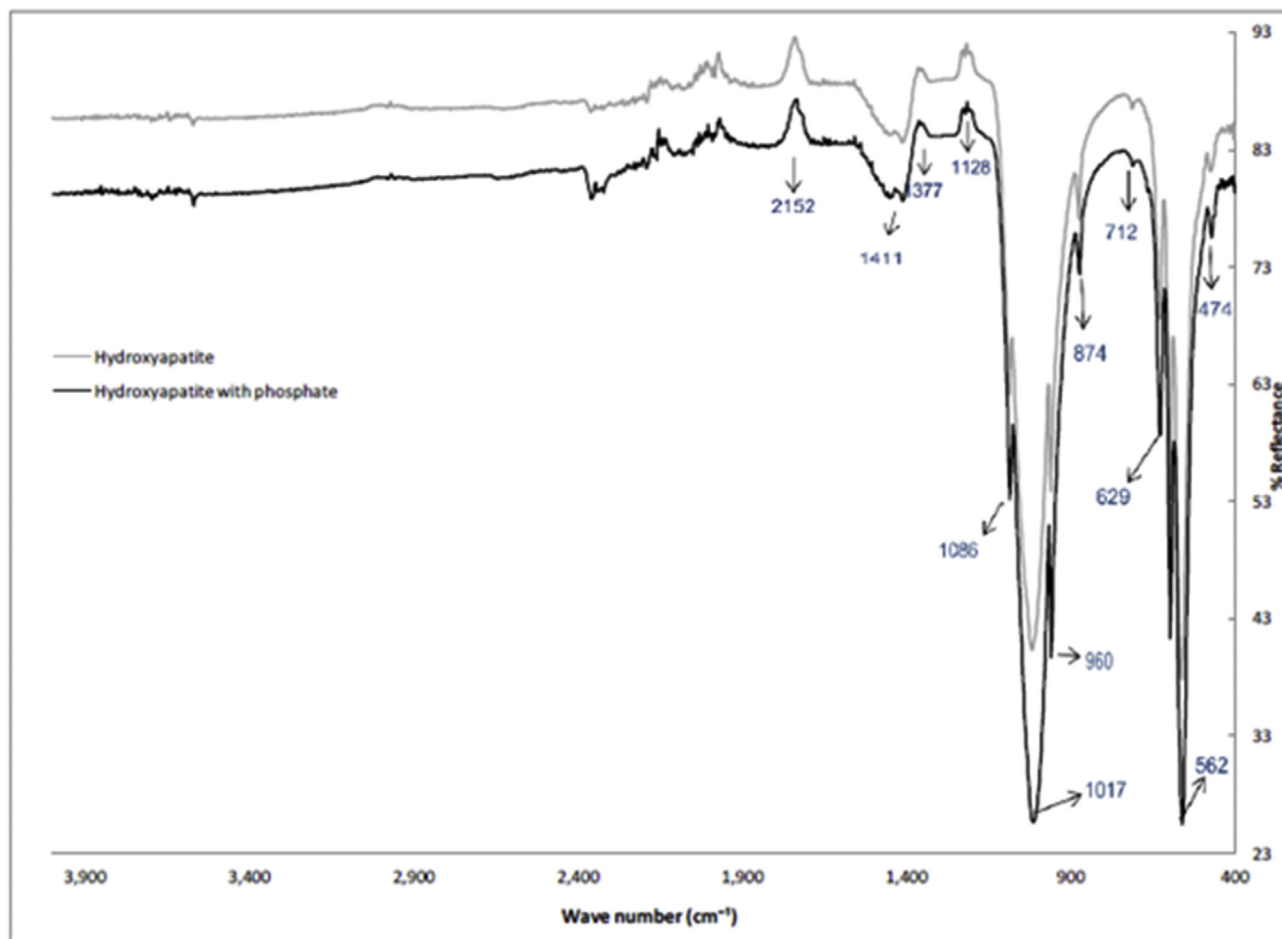
Fig. 7. IR spectra obtained for hydroxyapatite with and without phosphate adsorption.

as expected after adsorption of phosphate, the band at 1017 cm^{-1} moved to a lower wavenumber (1016 cm^{-1}) and the band at 960 cm^{-1} (stretching vibration of phosphate) increased intensity. The band at 874 cm^{-1} indicates the presence of carbonate ions (Wang et al., 2007). The CO$_3^{2-}$ band at 1411 cm^{-1} shifted to higher wavenumber (1452 cm^{-1}). The increase in the intensity of the above groups can be attributed to electrostatic attraction.

The results obtained analysing these spectra and the desorption achieved by solutions with high ionic strength suggest that the adsorption is predominantly produced by ionic exchange processes with both adsorbents. This is reinforced by the fact of fitting to a kinetic model of second order, based mainly on processes of chemisorptions, and the adjustment of the isothermal equilibrium data to the Langmuir monolayer model.

4. Conclusions

The investigation with systems that reduce the concentration of nutrients in water bodies is a good starting point for a solution to eutrophication problems.

According to the results of this study, it can be concluded that the presence of nitrate in the water to be treated, does not modify the phosphate adsorption onto dolomite nor onto hydroxyapatite. Both adsorbents could be useful for the treatment of water with phosphates in the presence of nitrate, which is usually the case. In this sense, hydroxyapatite proved to be the most efficient adsorbent, however, it showed a low percentage of desorption and few possibilities of reuse. Dolomite, on the other hand, allows a desorption of the adsorbed material that favours its reuse.

Equilibrium, kinetics, desorption and FTIR spectra studies indicate that mechanisms such as ion exchange are involved in the process.

These studies should continue with experiments to design the use and reuse cycles for both adsorbents in order to obtain a low cost process in continuous reactors.

The advance provided by the present work is given in two aspects. The main one is that for effluents with large amounts of nitrate and phosphate the phosphate could be selectively eliminated. This was demonstrated since the process studied for both adsorbents was not affected by the presence of nitrates. It is very important the study of interferences as they could reduce the efficiency of the process under study and even make it a useless process depending on the composition of the effluent to be treated. The other aspect is that more progress has been made in demonstrating that the mechanism by which the adsorption process occurs in this type of mineral adsorbents is that of ion exchange.

Nomenclature

C_e	concentration of the solution at equilibrium state, [mg L^{-1}]
t	time, [min]
q_e	amount of adsorbed species per unit mass of adsorbent at the equilibrium state, [mg g^{-1}]
q_d	amount of desorbed species per unit mass of adsorbent, [mg g^{-1}]
q_t	amount of adsorbed species per unit mass of adsorbent at the time t, [mg g^{-1}]
q_m	Langmuir parameter related to the maximum capacity of the adsorbent, [mg g^{-1}]
b	Langmuir parameter related to the energy of adsorption, [L mg^{-1}]
K_f	Freundlich parameter related to the adsorption capacity
n	Freundlich parameter related to the intensity of adsorption
k	velocity constant in the pseudo-first order model, [min^{-1}]
k_s	velocity constant in the pseudo-second order model, [M^{-1}min^{-1}]

References

Albadarin, A.B., Mangwandi, C., Al-Muhtaseb, A.H., Walker, G.M., Allen, S.J., Ahmad, M.N.M., 2012. Kinetic and thermodynamics of chromium ions adsorption onto low-cost dolomite adsorbent. Chem. Eng. J. 179, 193–202.

Anderson, D.M., Glibert, P.M., Burkholder, J.M., 2002. Harmful algal blooms and eutrophication: nutrient sources, composition, and consequences. Estuaries 25, 704–726.

Ansari, A., Singh Gill, S. (Eds.), 2014. Eutrophication: Causes, Consequences and Control, vol. 2. Springer, Netherlands.

Anthony, J.W., Bideaux, R.A., Bladh, K.W., Nichols, Monte C. (Eds.), 2011. Handbook of Mineralogy. Mineralogical Society of America, USA. http://www.handbookofmineralogy.org/.

APHA (American Public Health Association), AWWA (American Water Works Association), WEF(Water Environment Federation), 2012. In: Rice, E.W., Baird, R., Eaton, A., Clesceri, L. (Eds.), Standard Methods for the Examination of Waters and Wastewaters, twenty-second ed. American Public Health Association, Washington.

Bia, G., de Pauli, C.P., Borgnino, L., 2012. The role of Fe(III) modified montmorillonite on fluoride mobility: adsorption experiments and competition with phosphate. J. Environ. Manag. 100, 1–9.

Burkart, M.R., Stoner, J.D., 2002. Nitrate in aquifers beneath agricultural systems. Water Sci. Technol. 45, 19–28.

Cai, R., Wang, X., Ji, X., Peng, B., Tan, C., Huang, X., 2017. Phosphate reclaim from simulated and real eutrophic water by magnetic biochar derived from water hyacinth. J. Environ. Manag. 187, 212–219.

Cheung, K.C., Venkitachalam, T.H., 2000. Improving phosphate removal of sand infiltration system using alkaline fly ash. Chemosphere 41, 243–249.

Chiban, M., Soudani, A., Sinan, F., Persin, M., 2012. Wastewater treatment by batch adsorption method onto micro-particles of dried Withania frutescens plant as a new adsorbent. J. Environ. Manag. 95, S61–S65.

Coulibaly, L.S., Akpo, S., Yvon, J., Coulibaly, L., 2016. Fourier transform infra-red (FTIR) spectroscopy investigation, dose effect, kinetics and adsorption capacity of phosphate from aqueous solution onto laterite and sandstone. J. Environ. Manag. 183, 1032–1040.

Dabrowski, A., 2001. Adsorption from theory to practice. Adv. Colloid Interface Sci. 93, 135–224.

Deliyanni, E.A., Peleka, E.N., Lazaridis, N.K., 2007. Comparative study of phosphates removal from aqueous solutions by nanocrystalline akaganéite and hybrid surfactant-akaganéite. Sep. Purif. Technol. 52, 478–486.

Eaton, D.L., Gilbert, S.G., 2008. Principles of toxicology. In: Klaasen, C.D. (Ed.), Casarett and Doull's,Toxicology. The Basic Science of Poisons, seventh ed. Mc Graw − Hill, New York.

Freundlich, H., 1906. Adsorption in solutions (in German: die adsorption in lösungen). Z. Phys. Chem. 57, 385–470.

Fu, F., Wang, Q., 2011. Removal of heavy metal ions from wastewaters: a review. J. Environ. Manag. 92, 407–418.

Gregg, S.J., Sing, K.S.W., 1982. Adsorption Surface Area and Porosity. Academic Press Inc., London.

Hinz, C., 2001. Description of sorption data with isotherm equations. Geoderma 99, 225–243.

Ho, Y.S., McKay, G., 1999. Pseudo-second order model for sorption processes. Process Biochem. 34, 451–465.

Huang, W., Zhang, Y., Yi, D., 2017. Adsorptive removal of phosphate from water using mesoporous materials: a review. J. Environ. Manag. 193, 470–482.

Islam, M., Mishra, P.C., Patel, R., 2010. Physicochemical characterisation of hydroxyapatite and its application towards removal of nitrate from water. J. Environ. Manag. 91, 1883–1891.

Johir, M.A.H., Pradhan, M., Loganathan, P., Kandasamy, J., Vigneswaran, S., 2016. Phosphate adsorption from wastewater using zirconium (IV) hydroxide: kinetics, thermodynamics and membrane filtration adsorption hybrid system studies. J. Environ. Manag. 167, 167–174.

Karaca, S., Gürses, A., Ejder, M., Acikyildiz, M., 2006. Adsorptive removal of phosphate from aqueous solutions using raw and calcinated dolomite. J. Hazard. Mater. 128, 273–279.

Kumar, P., Ramakrishnan, K., Kirupha, S., Sivanesan, S., 2010. Thermodynamic and kinetic studies of cadmium adsorption from aqueoussolution onto rice husk. Braz. J. Chem. Eng. 27 (2), 347–355.

Lagergren, S., 1898. About the theory of so-called adsorption of soluble substances (in German: Zurtheorie der sogenannten adsorption gelosterstoffe), Supplement of the Royal Swedish Science Academiens Documents (in Swedish: Bihang Till Konglinga Svenska Vetenskaps Academiens Handlingar), Vol (in Swedish: Band) 24, Issue (in Swedish: Afdelning) 2, Article N° 4, pp 1–39.

Langmuir, I., 1918. The adsorption of gases on plane surfaces of glass, mica and platinum. J. Am. Chem. Soc. 40 (9), 1361–1403.

Liu, H., Sun, X., Yin, C., Hu, C., 2008. Removal of phosphate by mesoporous ZrO$_2$. J. Hazard. Mater. 151, 616–622.

Liu, Y., Xia, S., Yuanhua, D., Yijie, M., 2012. Removal of high-concentration phosphate by calcite: effect of sulfate and pH. Desalination 289, 66–71.

Liu, H., Wang, C., Liu, J., Wang, B., Sun, H., 2013. Competitive adsorption of Cd(II), Zn(II) and Ni(II) from their binary and ternary acidic systems using tourmaline. J. Environ. Manag. 128, 727–734.

Maier, G., Nimmo-Smith, R.J., Glegg, G.A., Tappin, A.D., Worsfold, P.J., 2009. Estuarine eutrophication in the UK: current incidence and future trends. Aquat. Conserv. Mar. Freshw. Ecosyst. 19, 43–56.

Manahan, S.E., 2001. Fundamentals of Environmental Chemistry. CRC Press, Boca Raton.

Mangwandi, C., Albadarina, A.B., Glocheuxa, Y., Walker, G.M., 2014. Removal of ortho-phosphate from aqueous solution by adsorption onto dolomite. J. Environ. Chem. Eng. 2, 1123–1130.

Miretzky, P., Saralegui, A., Fernández Cirelli, A., 2006. Simultaneous heavy metal removal mechanism by dead macrophytes. Chemosphere 62 (2), 247–254.

Monoj, K., Mondal, M.K., Mishra, G., Kumar, P., 2015. Adsorption of cadmium (II) and chromium (VI) from aqueous solution by waste marigold flowers. J. Sustain. Dev. Energy Water Environ. Syst. 3 (4), 405–415.

Nhapi, I., Banadda, N., Murenzi, R., Sekomo, C.B., Wali, U.G., 2011. Removal of heavy metals from industries waster using rice husks. Open Environ. Eng. J. 4, 170–180.

Nodeh, H., Sereshti, H., Afsharian, E., Nouri, N., 2017. Enhanced removal of phosphate and nitrate ions from aqueous media using nanosized lanthanum hydrous doped on magnetic grapheme nanocomposite. J. Environ. Manag. 197, 265–274.

Sepúlveda, A., Bustamante, F., Silvestre, J., Suárez, S., Orozco, N., 2008. Adsorbents for the removal of VOCs (in Spanish: adsorbentes para la eliminación de COVs). In: Elimination of atmospheric emissions of VOCs by Catalysis and Adsorption (in Spanish: Eliminación de emisiones atmosféricas de COVs por Catálisis y Adsorción), Chapter 7. CYTED, Madrid, España, pp. 50–59.

Silverstein, R.M., Webster, F.X., Kiemle, D., 2005. Spectrometric Identification of Organic Compounds. John Wiley & Son.

Vanreppelen, K., Schreurs, S., Kuppens, T., Thewys, T., Carleer, R., Yperman, J., 2013. Activated carbon by co-pyrolysis and steam activation from particle board and melamine formaldehyde resin: production, adsorption properties and techno economic evaluation. J. Sustain. Dev. Energy Water Environ. Syst. 1 (1), 41–57.

Von Sperling, M., 2007. Wastewater Characteristic, Treatment and Disposal. Federal University of Minas, Brazil.

Wang, A., Yin, H., Liu, D., Wu, H., Wada, Y., Ren, M., Xu, Y., Jiang, T., Cheng, X., 2007. Effects of organic modifiers on the size-controlled synthesis of hydroxyapatite nanorods. Appl. Surf. Sci. 253, 3311–3316.

Xu, H.Y., Yang, L., Wang, P., Liu, Y., Peng, M.S., 2008. Kinetic research on the sorption of aqueous lead by synthetic carbonate hydroxyapatite. J. Environ. Manag. 86, 319–328.

Yang, X.E., Wu, X., Hao, H.I., He, Z.I., 2008. Mechanisms and assessment of water eutrophication. J. Zhejiang Univ. Sci. B 9, 197–209.

Yang, Kun, Yan, Liang-guo, Yang, Yan-ming, Yu, Shu-jun, Shan, Ran-ran, Yu, Hai-qin, Zhu, Bao-cun, Du, Bin, 2014. Adsorptive removal of phosphate by Mg−Al and Zn−Al layered double hydroxides: kinetics, isotherms and mechanisms. Sep. Purif. Technol. 124, 36–42.